Overexpression of Epstein-Barr Virus-encoded microRNA-BART7 in Undifferentiated Nasopharyngeal Carcinoma

JIMMY YU-WAI CHAN*, WEI GAO*, WAI-KUEN HO, WILLIAM IGNACE WEI and THIAN-SZE WONG

Department of Surgery, The University of Hong Kong, China

Abstract. *Aim: To validate Epstein-Barr virus BamHI-A rightward transcript 7 microRNA (ebv-miR-BART7) expression in plasma from patients with nasopharyngeal carcinoma (NPC) and explore the oncogenic role of ebv-miR-BART7 in NPC cells. Patients and Methods: Plasma ebv-miR-BART7 levels were measured using real-time quantitative RT-PCR. Effects on cell proliferation, invasion, migration, and resistance to cisplatin were studied on NPC cells using real-time cell analyzer. Results: The plasma ebv-miR-BART7 level was significantly higher in patients with NPC in comparison with that from healthy individuals. The ebv-miR-BART7 was detectable in all the patient plasma samples and was independent of the EBV DNA level. In vitro expression of ebv-miR-BART7 enhanced proliferation, migration, and invasion of NPC cells. Furthermore, NPC cells expressing ebv-miR-BART7 were more resistant to cisplatin. High-throughput gene expression analysis suggested that ebv-miR-BART7 affects multiple cancer-related pathways. Conclusion: Our results indicate that plasma ebv-miR-BART7 could be used in NPC screening, especially in cases where EBV DNA is not detectable. The association of ebv-miR-BART7 with common oncogenic pathways suggests that ebv-miR-BART7 is a potential biomarker for undifferentiated NPC.*

Nasopharyngeal carcinoma (NPC) is a common type of head and neck cancer and is related to Epstein-Barr virus (EBV) infection. The major histological subtype is undifferentiated carcinoma, with high incidence in Southern China and Southeast Asia (1). Undifferentiated NPC is closely associated with Epstein-Barr virus, the first human virus found to be related to the development of human malignancy. EBV infection is an early event and EBV frequently exists in the early stages in dysplastic lesions and carcinoma *in situ* (2). Based on the consistent association of NPC and EBV, the genetic materials of EBV have been used in the diagnosis and screening of patients with NPC.

MicroRNAs (miRNA) are small non-protein-coding RNAs which regulate mRNA at the post-transcriptional level. miRNAs are small (19-22 or 19-25 nucleotides) epigenetic regulators (3). miRNAs bind to their target mRNAs in a partial or complete complementary manner. They regulate gene expression by promoting target mRNA degradation and/or hindering mRNA translation (4). The EBV genome contains two major clusters, *Bam*HI fragment H rightward open reading frame 1 (BHRF1) and *Bam*HI-A rightward transcript (BART), coding for 25 precursors and 44 mature viral-encoded miRNA. ebv-miR-BART7 (MI0003729) is a viral-encoded miRNA, which is highly expressed in undifferentiated NPC cells latently infected with EBV. ebv-miR-BART7 was discovered in 2006, however, the extent of ebv-miR-BART7 expression in NPC was not explored at that time (5, 6). Mature ebv-miR-BART7 (MIMAT0003416) is a single-stranded molecule containing 22 nucleotides (5-caucauaguccaguguccaggg-3). A recent study using next-generation sequencing confirmed that ebv-miR-BART7 was highly expressed in NPC cells, suggesting that it might have an oncogenic role (7).

Here, we explored the use of circulating ebv-miR-BART7 in NPC screening and compared it with the circulating EBV DNA. Furthermore, we examined the role of ebv-miR-BART7 in the genesis of NPC cells and explored the potential functional pathways affected by ebv-miR-BART7.

Patients and Methods

Patient samples. Peripheral blood samples were obtained from patients with NPC at the Department of Surgery, The University of Hong Kong, Queen Mary Hospital, Hong Kong. Peripheral blood samples were collected from 41 patients with primary NPC, 21 with recurrent NPC and from 21 healthy volunteers. The patients with primary NPC included 34 males and seven females, their age ranging from 23-79 years. There were six patients with T1 stage

*These Authors contributed equally to this study.

Correspondence to: Thian-Sze Wong, Queen Mary Hospital, 102 Pokfulam Road, Hong Kong SAR, China. Tel: +852 28199604, Fax: +852 28553464, e-mail: thiansze@graduate.hku.hk

Key Words: EBV, ebv-miR-BART7, NPC screening, oncogenic role, cancer-related pathways, nasopharyngeal carcinoma.

disease, 24 with T2, 10 with T3 and one with T4. The patients with recurrent NPC included 17 males and four females, aged from 29-75 years; there were seven patients with T1 disease, three with T2, seven with T3, and four with T4.

Cell cultures. NPC cell lines HK1 (Hong Kong, China) and HONE1 (Hunan, China) were maintained in RPMI-1640 medium (Gibco, Grand Island, NY, USA) supplemented with 10% fetal bovine serum (Gibco). HK1 is derived from well-differentiated squamous carcinoma (8); HONE1 is derived from poorly differentiated squamous carcinoma (9).

Immunocytochemistry. NPC cells were washed with PBS and fixed with 2% paraformaldehyde overnight. The nucleus was stained by blue-fluorescent 4',6-Diamidino-2-Phenylindole (DAPI) (Invitrogen, Grand Island, NY, USA); F-actin was labeled in red with Alexa Fluor® 635 phalloidin (Invitrogen, Grand Island, NY, USA). The morphologies of HONE1 and HK1 transfected with 1.5 nM ebv-miR-BART7 (BART7) mimic or negative control siRNA were observed.

RNA extraction and real-time quantitative RT-PCR analysis. Total RNA was extracted with TRIZOL (Invitrogen) following the manufacturer's protocol. RNA was converted to cDNA using High-Capacity cDNA Reverse Transcription Kit (Applied Biosystems, Carlsbad, California, USA). Transcripts levels of *ebv-miR-BART7* and *U6* control snRNA were measured by TaqMan Gene Expression Assays (Applied Biosystems) using a LightCycler® 480 (Roche Applied Science, Indianapolis, IN, USA).

EBV DNA quantification. Absolute EBV DNA quantification was performed using LightMix® Kit for the detection of EBV (TIB MOLBIOL, Berlin, Germany). EBV DNA purified from 200 μl plasma by High Pure Viral Nucleic Acid Kit (Roche Applied Science) was amplified using a LightCycler® 480 (Roche Applied Science). Absolute EBV quantification was calculated using a standard curve derived from 10^1-10^6 copies of EBV DNA.

Proliferation, migration and invasion assay. Proliferation assay was performed on E-Plate 16 using a RTCA DP instrument (Roche Applied Science). Real-time migration and invasion monitoring was performed using CIM-Plate 16 on a RTCA DP instrument. HONE1 and HK1 transfected with 1.5 nM ebv-miR-BART7 mimic or negative control siRNA using Hiperfect transfection reagent (QIAGEN, Valencia, CA, USA) were seeded on E-Plate 16 or CIM-Plate 16. For invasion assay, the upper chamber of CIM-Plate 16 was coated with Matrigel (1:30 dilution; BD Biosciences, San Jose, California, USA) for 4 hours at 37˚C. The culture medium containing 10% FBS was added to the lower chamber as a chemo-attractant.

Cisplatin-resistance assay. After transfection with 1.5 nM ebv-miR-BART7 mimic or negative control siRNA for 72 hours, HONE1 and HK1 were harvested and seeded on E-plate 16. After 26 hours, cisplatin was added to the medium at a final concentration of 17 μM, followed by real-time cell index monitoring for 23 hours. The cell index of NPC cells transfected with BART7 mimic was compared to that of NPC cells transfected with negative control siRNA.

Microarray analysis. The RNA quality assessment, gene expression microarray and data analysis were carried out at the Genome Research Centre of the University of Hong Kong. GeneChip Human Genome U133 Plus 2.0 Array (Affymetrix, Santa Clara, CA, USA) was used for global gene expression profiling. Microarray data analysis was performed with GeneSpring GX version 10.0 (Agilent Technologies, Santa Clara, CA, USA). Median normalization of log2-transformed data was used. The differentially expressed genes were evaluated by DAVID Bioinformatics Resources 6.7 (http://david.abcc.ncifcrf.gov/home.jsp).

Statistical analysis. Statistical analysis was performed with SPSS V16.0 (Armonk, New York, USA).

Results

Circulating ebv-miR-BART7 levels in patients with NPC and healthy individuals. Figure 1A shows the serological ebv-miR-BART7 levels in our cohort. Patients with primary NPC had significantly higher plasma ebv-miR-BART7 levels in comparison with the healthy individuals ($p<0.001$, Mann-Whitney *U*-test) (Figure 1A). Figure 1A also shows the receiver operating characteristic (ROC) analysis for circulating ebv-miR-BART7 in our cohort. The area under the curve (AUC) was 0.81 (Figure 1A).

Comparison of circulating EBV DNA and ebv-miR-BART7 in NPC patients. EBV DNA was detected in 18 out of 41 (44%) plasma samples of patients with NPC (Figure 1B). In healthy plasma, the EBV DNA level was below the detectable level in all 21 cases (Figure 1B). The plasma EBV DNA level was significantly higher in patients with primary NPC in comparison with the healthy controls ($p=0.024$, Mann-Whitney *U*-test) (Figure 1B). In comparison, ebv-miR-BART7 was detected in all 41 (100%) primary NPC cases and the ebv-miR-BART7 level was independent of the circulating EBV DNA level (Figure 1C). Furthermore, a high level of ebv-miR-BART7 was observed in both serologically EBV DNA-positive ($p<0.001$, Mann-Whitney *U*-test) and -negative ($p=0.001$, Mann-Whitney *U*-test) primary NPC cases in comparison with healthy controls (Figure 1C).

Circulating ebv-miR-BART7 and EBV DNA level in recurrent NPC patients. In comparison with primary NPC, patients with recurrent NPC had a lower serological ebv-miR-BART7 level ($p<0.001$, Mann-Whitney *U*-test) (Figure 1D). Although the median serological ebv-miR-BART7 level was higher in patients with recurrent NPC in comparison with the healthy controls, no statistically significant difference was observed. Both primary NPC and recurrent NPC had significantly higher plasma EBV DNA levels in comparison with the healthy controls (Figure 1E).

Effects of ebv-miR-BART7 on proliferation, migration, and invasion of NPC cells. To explore the functional role of ebv-miR-BART7 on NPC cells, ectopic expression of ebv-miR-

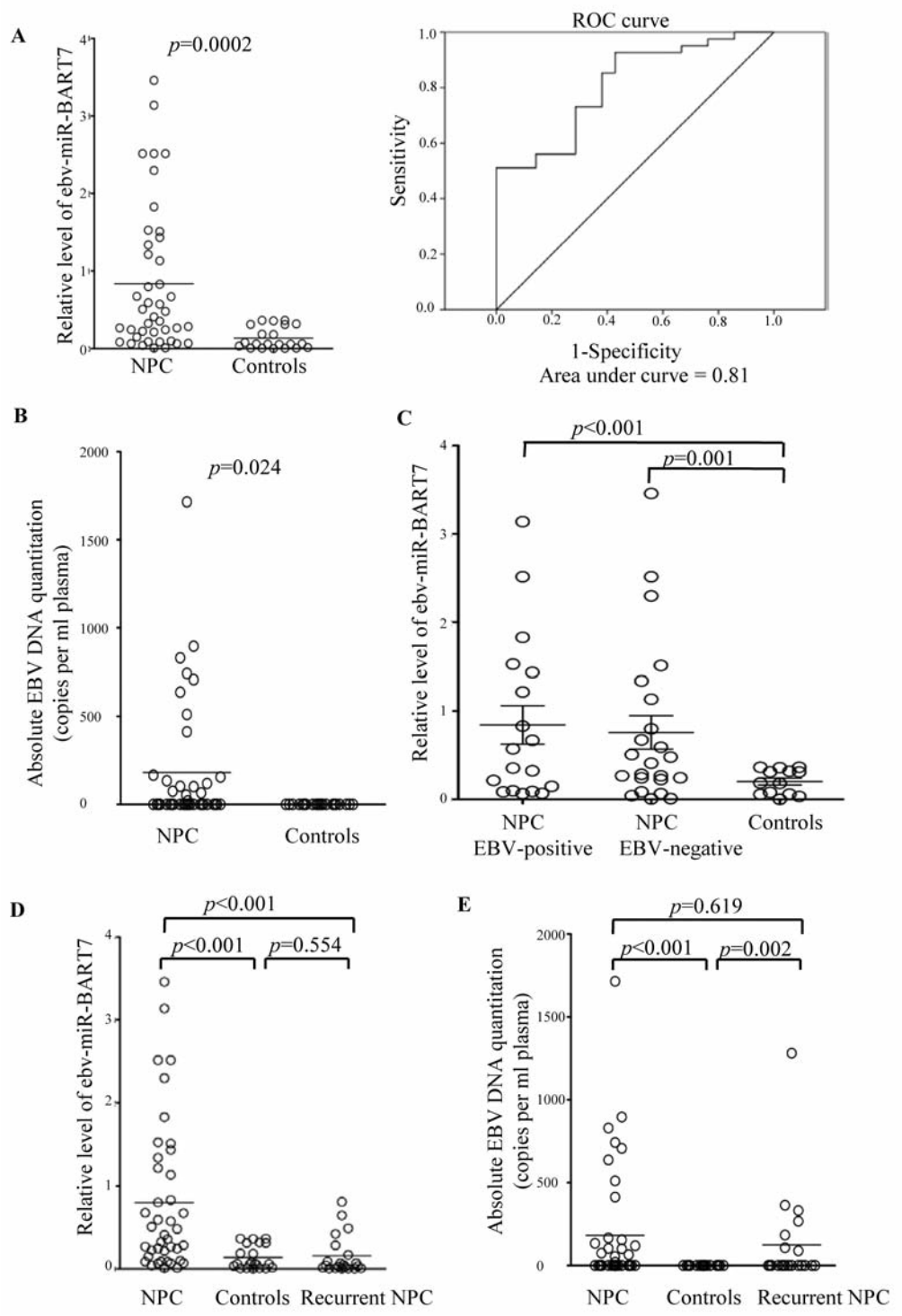

Figure 1. *Relative ebv-miR-BART7 expression level and absolute EBV DNA level in plasma from patients with NPC, recurrent NPC and healthy controls. A: Relative ebv-miR-BART7 expression level and receiver operating characteristic (ROC) curve for plasma samples from 41 NPC and 21 healthy controls. The relative expression level of ebv-miR-BART7 was normalized to U6 snRNA by qPCR analysis and the data are displayed as* $2^{-\Delta Ct}$. *B: Absolute EBV DNA level in plasma from 41 NPC cases and 21 healthy controls. Absolute EBV quantitation was derived from a standard curve of 101-106 copies of EBV DNA by qPCR analysis. C: Relative ebv-miR-BART7 expression level in plasma in EBV-positive and EBV-negative NPC and healthy controls. D: Relative ebv-miR-BART7 expression level in plasma from 41 NPC, 21 healthy controls and 21 recurrent NPC cases. E: Absolute EBV DNA level in plasma from 41 NPC, 21 healthy controls and 21 recurrent NPC cases. The difference between plasma in cases and controls was calculated using the Mann-Whitney test.*

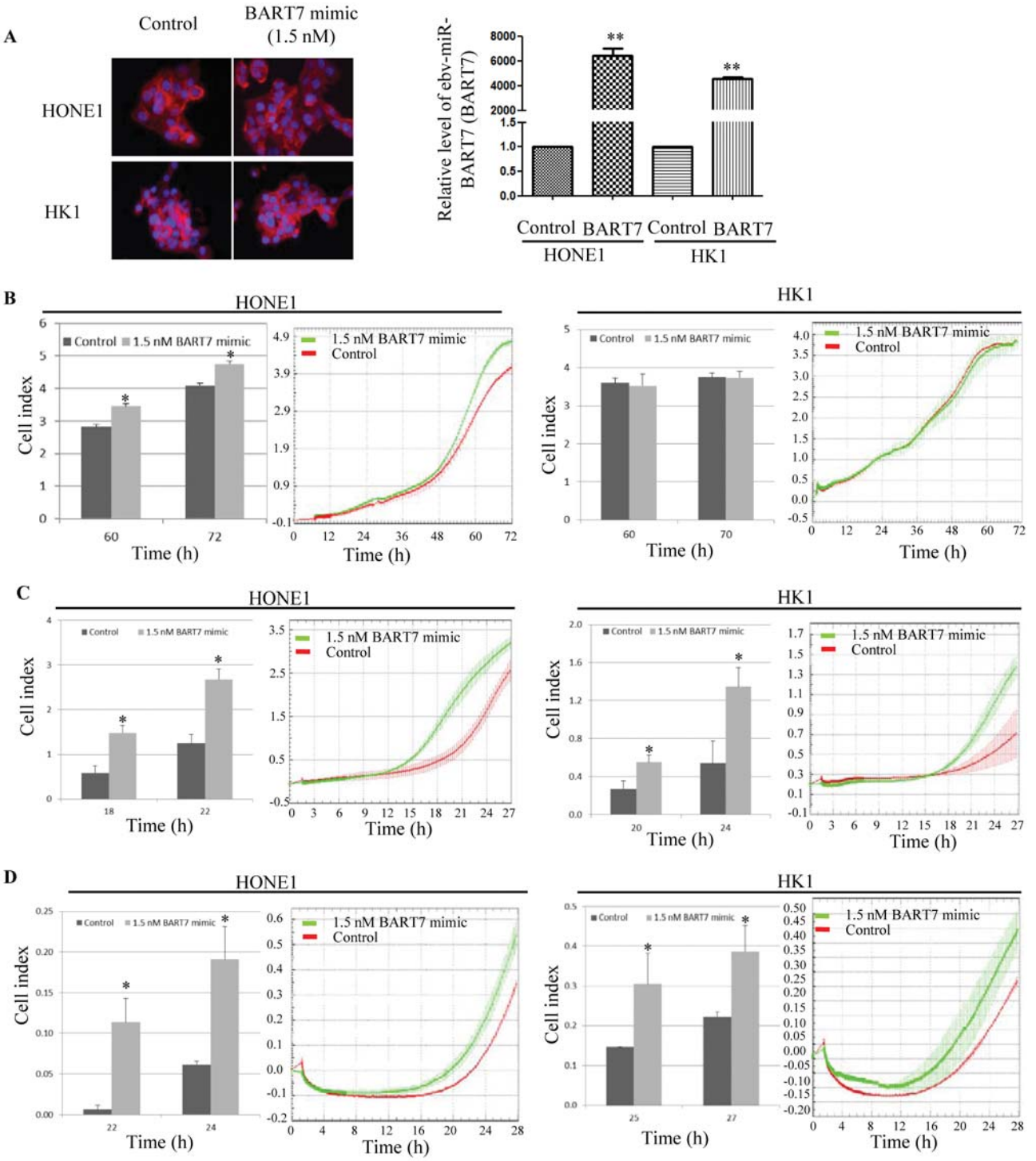

Figure 2. *Effect of ebv-miR-BART7 overexpression on proliferation (B), migration (C) and invasion (D) of HONE1 and HK1 cell lines. A: Immunocytochemistry and relative expression of ebv-miR-BART7 in HONE1 and HK1 cell lines transfected with ebv-miR-BART7 (BART7) mimic or negative control siRNA for 72 hours. Magnification, ×400. B: For the proliferation assay, HONE1 and HK1 were transfected with BART7 mimic or negative control siRNA and seeded on E-plate16. The live cell index was monitored for 72 hours. C: For the migration assay, HONE1 and HK1 cells transfected with BART7 mimic or negative control siRNA for 72 hours were harvested and seeded on CIM-plate 16. The live cell index was monitored for 27 hours. D: For the invasion assay, the upper chamber of CIM-Plate 16 was coated with Matrigel. The culture medium containing 10% FBS was added to the lower chamber as a chemo-attractant. HONE1 and HK1 transfected with BART7 mimic or negative control siRNA for 72 hours were harvested and seeded on CIM-plate 16. The live cell index was monitored for 28 hours. The experiments were carried out in duplicate. Bar indicates SD. *p<0.05 and **p<0.01 by t-test.*

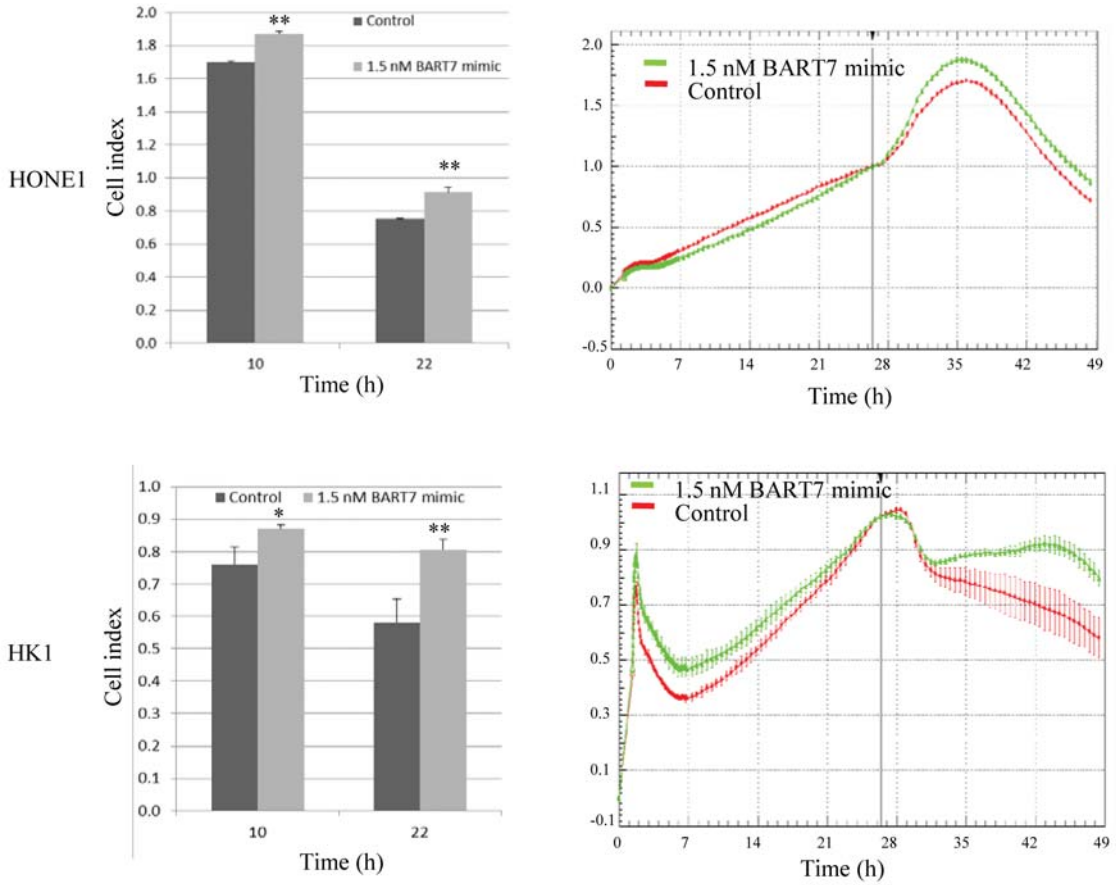

Figure 3. *Effect of ebv-miR-BART7 overexpression on the response of HONE1 and HK1 cell lines to cisplatin treatment. After transfection with BART7 mimic or negative control siRNA for 72 hours, HONE1 and HK1 were harvested and seeded on E-plate16. After 26 hours, cisplatin was added to the medium at a final concentration of 17 μM, followed by a real-time cell index monitoring for 23 hours. The cell index was normalized using the time point that cisplatin was added to the medium. The experiments were carried out in triplicate. Bar indicates SD. *p<0.05 and **p<0.01 by t-test.*

BART7 was performed on 2 EBV-negative NPC cell lines HONE1 and HK1. Overexpression of ebv-miR-BART7 was observed in HONE1 and HK1 transfected with ebv-miR-BART7 mimic (Figure 2A). In the presence of ebv-miR-BART7, HONE1 demonstrated a significant increase in the rate of proliferation (Figure 2B), migration (Figure 2C) and invasion (Figure 2D). For HK1, in the presence of mature ebv-miR-BART7, we only observed an increase in migration (Figure 2C) and invasion (Figure 2D). ebv-miR-BART7 expression had no significant effects on the proliferation rate of HK1 cells (Figure 2B).

Cisplatin sensitivity of ebv-miR-BART7-expressing NPC cells. To examine the role of ebv-miR-BART7 in response to cisplatin treatment, we transfected the NPC cell lines HONE1 and HK1 with ebv-miR-BART7 mimic and exposed the cells to cisplatin. Figure 3 shows that ebv-miR-BART7-expressing cells were more resistant to cisplatin in comparison with the mock control. Both HONE1 and HK1 cells demonstrated significant resistance to cisplatin in the presence of ebv-miR-BART7.

Functional pathways affected by ebv-miR-BART7 in the NPC HONE1 cells. We examined the global gene expression alterations in the undifferentiated NPC cells HONE1 induced by ebv-miR-BART7 with microarray analysis. With a fold-change cut-off of 3 and $p<0.05$, 625 genes were found to be differentially expressed in the presence of ebv-miR-BART7 (Table I). Pathway analysis indicated that ebv-miR-BART7 expression affects the signaling pathway of calcium ($p=0.003$) and of the immune system ($p=0.013$), ionotropic glutamate receptor ($p=0.016$), ATP-binding cassette (ABC) transporters ($p=0.019$), nuclear receptors in lipid metabolism and toxicity ($p=0.029$), transforming growth factor (TGF)-

Table I. *Gene Ontology classification of 625 differentially expressed genes (p<0.05, fold-change=3) by DAVID Bioinformatics Resources 6.7.*

Function name	Number of genes	*p*-Value
Biological process		
Regulation of cell adhesion	14	3.73E-04
Positive regulation of cell migration	11	4.91E-04
Positive regulation of glucose import	6	5.21E-04
Positive regulation of glucose transport	6	5.21E-04
Chemical homeostasis	31	6.42E-04
Regulation of cell migration	15	9.56E-04
Positive regulation of locomotion	11	0.001
Positive regulation of cell motion	11	0.001
Regulation of locomotion	16	0.001
Lymphocyte differentiation	11	0.002
Bone development	12	0.002
Leukocyte activation	18	0.002
Negative regulation of cell adhesion	7	0.002
Forebrain development	13	0.003
Leukocyte differentiation	12	0.003
Tissue regeneration	6	0.003
Prepulse inhibition	4	0.003
Immune response	34	0.003
Ossification	11	0.003
Regulation of cell motion	15	0.003
Cell fate commitment	12	0.003
Regulation of glucose import	6	0.004
Telencephalon development	8	0.004
Behavioral interaction between organisms	6	0.004
Regulation of glucose transport	6	0.004
Lymphocyte activation	15	0.004
Cell activation	19	0.004
Negative regulation of cell-substrate adhesion	4	0.004
Growth	14	0.004
Cellular cation homeostasis	17	0.006
Cell motion	26	0.006
Hemopoiesis	16	0.008
Negative regulation of transcription from RNA polymerase II promoter	17	0.009
Phospholipid homeostasis	3	0.009
Regulation of cell-matrix adhesion	5	0.010
Dicarboxylic acid transport	4	0.011
Enzyme linked receptor protein signaling pathway	20	0.012
Blood vessel development	16	0.012
Skeletal system development	19	0.012
Myotube differentiation	4	0.013
Regulation of ATPase activity	4	0.013
Startle response	4	0.013
Response to inorganic substance	14	0.013
Cellular ion homeostasis	21	0.013
Regulation of cell-substrate adhesion	6	0.013
Positive regulation of cellular biosynthetic process	33	0.014
Vasculature development	16	0.014
Cell motility	18	0.015
Localization of cell	18	0.015
Muscle cell differentiation	10	0.015
Cellular chemical homeostasis	21	0.016
Neuron differentiation	23	0.017
T-Cell differentiation	7	0.017
Cation homeostasis	17	0.017
Positive regulation of biosynthetic process	33	0.017
Ion homeostasis	22	0.017
B-Cell differentiation	6	0.017
Regulation of transcription, DNA-dependent	69	0.017

Table I. *Continued*

Table I. *Continued*

Function name	Number of genes	*p*-Value
T-Cell activation	10	0.018
Regulation of actin cytoskeleton organization	8	0.018
Response to corticosteroid stimulus	8	0.018
Hemopoietic or lymphoid organ development	16	0.018
Neuron development	19	0.018
Response to organic substance	34	0.019
Regulation of establishment of protein localization to plasma membrane	3	0.019
Aspartate transport	3	0.019
Regulation of lipase activity	8	0.019
Negative regulation of RNA metabolic process	20	0.019
Smooth muscle contraction	5	0.020
Behavior	24	0.020
Regulation of RNA metabolic process	70	0.020
Cellular metal ion homeostasis	13	0.020
Response to metal ion	10	0.020
Cell projection organization	20	0.021
T-Cell selection	4	0.021
Immune effector process	10	0.021
Regulation of actin filament-based process	8	0.021
Regeneration	7	0.022
Cell surface receptor linked signal transduction	61	0.023
Regulation of phospholipase activity	7	0.023
Response to hormone stimulus	20	0.024
Cellular di-, tri-valent inorganic cation homeostasis	14	0.024
Negative regulation of B-cell proliferation	3	0.025
Cell migration	16	0.025
Glial cell differentiation	6	0.026
Positive regulation of hydrolase activity	12	0.026
Actin filament organization	7	0.026
Regulation of muscle contraction	7	0.026
Cell adhesion	32	0.026
Biological adhesion	32	0.027
Metal ion homeostasis	13	0.027
Phospholipid catabolic process	4	0.027
Immune system development	16	0.028
Homeostatic process	34	0.029
Regulation of apoptosis	36	0.029
Positive regulation of apoptosis	2	0.029
Negative regulation of transcription, DNA-dependent	19	0.031
Ventricular cardiac muscle morphogenesis	4	0.031
Positive regulation of ATPase activity	3	0.031
Positive T-cell selection	3	0.031
Cellular lipid catabolic process	7	0.031
Cyclic nucleotide metabolic process	5	0.031
Positive regulation of programmed cell death	22	0.031
Response to endogenous stimulus	21	0.032
Positive regulation of cell death	22	0.033
Regulation of programmed cell death	36	0.033
Cell-cell signaling	28	0.033
Positive regulation of epithelial cell proliferation	5	0.034
Regulation of cell death	36	0.035
Di-, tri-valent inorganic cation homeostasis	14	0.036
Blood vessel morphogenesis	13	0.038
Negative regulation of cell-matrix adhesion	3	0.038
Skeletal muscle regeneration	3	0.038
Response to acid	4	0.039
Response to wounding	25	0.040
Osteoblast differentiation	5	0.043
Neuromuscular process	6	0.043

Table I. *Continued*

Table I. *Continued*

Function name	Number of genes	*p*-Value
Negative regulation of immune system process	7	0.045
Positive regulation of nitrogen compound metabolic process	29	0.046
Regulation of transcription from RNA polymerase II promoter	32	0.047
Regulation of lymphocyte proliferation	7	0.048
Positive regulation of transport	13	0.049
Regulation of mononuclear cell proliferation	7	0.049
Regulation of leukocyte proliferation	7	0.049
Molecular function		
Phosphoric diester hydrolase activity	11	3.50E-04
Actin binding	23	8.67E-04
3',5'-cyclic-nucleotide phosphodiesterase activity	6	9.63E-04
Cyclic-nucleotide phosphodiesterase activity	6	0.001
Sodium:dicarboxylate symporter activity	4	0.004
Acidic amino acid transmembrane transporter activity	4	0.006
Cytoskeletal protein binding	28	0.007
Calcium:cation antiporter activity	3	0.010
Transcription factor activity	44	0.013
Dicarboxylic acid transmembrane transporter activity	4	0.014
Alkali metal ion binding	15	0.015
Protein dimerization activity	28	0.018
Solute:sodium symporter activity	6	0.024
Symporter activity	10	0.031
Sodium ion binding	9	0.032
3',5'-cyclic-AMP phosphodiesterase activity	3	0.034
Transcription regulator activity	61	0.034
Organic acid:sodium symporter activity	4	0.039
Apolipoprotein binding	3	0.041
Cytokine activity	12	0.044
Calmodulin binding	10	0.045
L-Glutamate transmembrane transporter activity	3	0.049

signaling pathway (p=0.035), dilated cardiomyopathy (p=0.037,) opioid signaling (p=0.04), and metabolism of lipids and lipoproteins (p=0.045) (Table II).

Discussion

EBV DNA is now regarded as a molecular marker for NPC diagnosis and screening. The major drawback is that EBV DNA is not present in all patients with NPC. Regional data suggested that a subgroup of patients with NPC is serological negative for circulating EBV DNA (10). Yuan *et al*. demonstrated that EBV DNA is present only in 67% of NPC cases (11). In a study using mixed plasma and serum samples, 41% (69/176) of patients with NPC were serologically negative for EBV DNA (12). In low-risk areas, such as Europe, EBV DNA is also not an absolute marker. Patients with EBV-encoded small RNA (EBER)-negative NPC had no detectable EBV DNA in their circulation. Thus, in cases where both EBV antibody and EBV DNA are lacking, there will be no suitable marker available for NPC detection/monitoring.

As shown in our results, both patients with NPC and healthy individuals had detectable circulating ebv-miR-BART7 in the plasma. Similar to EBV DNA, ebv-miR-BART7 was significantly higher in patients with NPC in comparison with the healthy controls. To test our hypothesis that ebv-miR-BART7 could be used as a serological marker in cases where no circulating EBV DNA is found, we analyzed the plasma ebv-miR-BART7 levels according to the detection rate of EBV DNA in the plasma samples. High plasma ebv-miR-BART7 was detected in patients with NPC and the circulating level is independent of the level of circulating EBV DNA. Intra-categorical analysis revealed that ebv-miR-BART7 levels are similar in patients with NPC regardless of serological EBV DNA detection. Furthermore, ROC analysis indicated that serological ebv-miR-BART7 is useful to differentiate patients with NPC from healthy individuals (p=0.0002).

To examine the functional role of ebv-miR-BART7 in NPC, we transfected the ebv-miR-BART7 mimic into the NPC-derived cell lines and examined the behavioral

Table II. *Pathway analysis of 625 differentially expressed genes (p<0.05, fold-change=3) by DAVID Bioinformatics Resources 6.7.*

Pathway	Name	Number of genes	*p*-Value	Associated genes
KEGG	Calcium signaling pathway	15	0.003	215340_at (adenylate cyclase 1); 206251_s_at (arginine vasopressin receptor 1A); 1555993_at (calcium channel, voltage-dependent, L type, alpha 1D subunit); 240650_at (calcium channel, voltage-dependent, R type, alpha 1E subunit); 211174_s_at (cholecystokinin A receptor); 214652_at (dopamine receptor D1); 237938_at (epidermal growth factor receptor); 232499_at (inositol 1,4,5-trisphosphate 3-kinase B); 208396_s_at (phosphodiesterase 1A, calmodulin-dependent); 216869_at (phosphodiesterase 1C); 221037_s_at (solute carrier family 25); 1568859_a_at (solute carrier family 8); 210637_at (tachykinin receptor 1); 205388_at (troponin C type 2); 214053_at (v-erb-a erythroblastic leukemia viral oncogene homolog 4)
KEGG	ABC transporters	6	0.019	1565776_at (ATP-binding cassette, sub-family A, member 1); 235335_at (ATP-binding cassette, sub-family A, member 9); 209994_s_at (ATP-binding cassette, sub-family B, member 1); 208288_at (ATP-binding cassette, sub-family B, member 11); 240717_at (ATP-binding cassette, sub-family B, member 5); 216418_at (ATP-binding cassette, sub-family D, member 1)
KEGG	Dilated cardiomyopathy	8	0.037	215340_at (adenylate cyclase 1); 1555993_at (calcium channel, voltage-dependent, L type, alpha 1D subunit); 206996_x_at (calcium channel, voltage-dependent, beta 1 subunit); 234750_at (calcium channel, voltage-dependent, gamma subunit 8); 209540_at (insulin-like growth factor 1); 205885_s_at (integrin, alpha 4); 205589_at (myosin, light chain 3, alkali); 1558532_at (tropomyosin 1)
BIOCARTA	Nuclear receptors in lipid metabolism and toxicity	5	0.029	1565776_at (ATP-binding cassette, sub-family A, member 1); 209994_s_at (ATP-binding cassette, sub-family B, member 1); 208288_at (ATP-binding cassette, sub-family B, member 11); 207773_x_at (cytochrome P450, family 3, subfamily A, polypeptide 43); 208412_s_at (retinoic acid receptor, beta)
PANTHER	Ionotropic glutamate receptor pathway	7	0.016	215830_at (SH3 and multiple ankyrin repeat domains 2); 240650_at (calcium channel, voltage-dependent, R type, alpha 1E subunit); 234750_at (calcium channel, voltage-dependent, gamma subunit 8); 233220_at (glutamate receptor, ionotropic, N-methyl-D-aspartate 3A); 1558009_at (solute carrier family 1, member 2); 210923_at (solute carrier family 1, member 7); 1554592_a_at (solute carrier family 1, member 6)
PANTHER	TGF-beta signaling pathway	11	0.035	216785_at (FK506 binding protein 1B, 12.6 kDa); 238394_at (SMAD specific E3 ubiquitin protein ligase 2); 210838_s_at (activin A receptor type II-like 1); 207866_a (bone morphogenetic protein 8a); 236256_at (forkhead box A1); 214520_at forkhead box C2); 1555352_at (forkhead box P2); 220053_at (growth differentiation factor 3); 214326_x_at (jun D proto-oncogene); 206012_at (left-right determination factor 2); 207145_at (myostatin)
REACTOME	Signaling in immune system	16	0.013	215332_s_at (CD8b molecule); 211395_x_at (Fc fragment of IgG, low affinity IIb, receptor for CD32; Fc fragment of IgG, low affinity IIc, receptor for CD32); 205572_at (angiopoietin 2); 1568730_at (caspase recruitment domain family, member 11); 202312_s_at (collagen, type I, alpha 1); 1558176_at (immunoglobulin lambda variable 7-46); 233545_at (inositol polyphosphate-5-phosphatase, 145kDa); 205885_s_at (integrin, alpha 4); 217296_at (killer cell immunoglobulin-like receptor, two domains, long cytoplasmic tail, 2); 210680_s_at (mannan-binding lectin serine peptidase 1); 243414_at (peptidylprolyl isomerase-like 2); 239476_at (phosphoinositide-3-kinase, regulatory subunit 1, alpha); 216207_x_at (similar to hCG26659); 222952_s_at (toll-like receptor 7); 221284_s_at (v-src sarcoma viral oncogene omolog, avian); 203868_s_at (vascular cell adhesion molecule 1)
REACTOME	Opioid signaling	7	0.040	215340_at (adenylate cyclase 1); 214547_at (adenylate cyclase 10); 208396_s_at (phosphodiesterase 1A, calmodulin-dependent); 216869_at (phosphodiesterase 1C, calmodulin-dependent 70kDa); 211901_s_at (phosphodiesterase 4A, cAMP-specific); 211840_s_at (phosphodiesterase 4D, cAMP-specific); 206803_at (prodynorphin)
REACTOME	Metabolism of lipids and lipoproteins	10	0.045	1565776_at (ATP-binding cassette, sub-family A, member 1); 208288_at (ATP-binding cassette, sub-family B, member 11); 216418_at (ATP-binding cassette, sub-family D, member 1); 1552615_at (acetyl-Coenzyme A carboxylase beta); 243283_at (carnitine O-octanoyltransferase); 206210_s_at (cholesteryl ester transfer protein, plasma); 214610_at (cytochrome P450, family 11, subfamily B, polypeptide 1); 1563360_at (cytochrome P450, family 19, subfamily A, polypeptide 1); 1566126_at (fatty acid binding protein 6, ileal), 216390_at (lecithin-cholesterol acyltransferase)

ABC: ATP-binding cassette; TGF: transforming growth factor.

changes. HONE1 was originally derived from NPC tissue which was EBV positive. Prolonged culture and continuous passaging resulted in the loss of EBV genome in NPC HONE1 cell. In contrast, HK1 is derived from differentiated NPC which was originally EBV negative. Interestingly, ebv-miR-BART7 had a positive effect on all the examined cancer cell properties, especially in the undifferentiated NPC cell line HONE1. ebv-miR-BART7 increased cell proliferation, promoted cell migration and increased invasion. In addition, in the presence of ebv-miR-BART7, both NPC cell lines became more resistant to cisplatin, a common chemotherapeutic agent used in NPC treatment. The results indicated that ebv-miR-BART7 plays a critical functional role and has an augmentative impact on the aggressive phenotype in NPC.

The gene products of EBV can alter somatic gene expression by controlling the biogenesis machinery of the host cells (13). We therefore suggested that the ebv-miR-BART7 would also have the same effect and control the transcriptome at post-transcriptional levels. In view of the fact that ebv-miR-BART7 induced multiple behavioral changes in NPC cells, we tried to identify the relevant biological pathways with microarray analysis and performed functional grouping of the differentially expressed genes using DAVID. Pathway analysis revealed that ebv-miR-BART7 alters multiple cancer-related pathways in undifferentiated NPC cells, implying that ebv-miR-BART7 is a critical player in the pathogenesis of undifferentiated NPC.

In conclusion, our results confirmed that ebv-miR-BART7 is highly expressed in NPC and the result is concordant with other similar studies. ebv-miR-BART7 is a critical viral oncomir as it can affect a myriad of functional pathways of NPC cells. By identifying suitable cut-off levels in further and larger sample sets, ebv-miR-BART7 might possibly be used in serological monitoring of patients with NPC, especially in cases where serological EBV DNA is not applicable. Further studies are warranted to explore the clinical use of EBV-derived miRNA in diagnosis, prognosis and follow-up management of patients with undifferentiated NPC.

Acknowledgements

This study was supported by Seed Funding of Basic Research, The University of Hong Kong, Li Shu Pui Professorship, The University of Hong Kong, Hong Kong Area of Excellent Scheme and Hong Kong UGC.

References

1 Wei WI and Sham JS: Nasopharyngeal carcinoma. Lancet *365*: 2041-2054, 2005.
2 Pathmanathan R, Prasad U, Sadler R, Flynn K and Raab-Traub N: Clonal proliferations of cells infected with Epstein-Barr virus in preinvasive lesions related to nasopharyngeal carcinoma. N Engl J Med *333*: 693-698, 1995.
3 Ambros V: The functions of animal microRNAs. Nature *431*: 350-355, 2004.
4 Bushati N and Cohen SM: microRNA functions. Annu Rev Cell Dev Biol *23*: 175-205, 2007.
5 Cai X, Schäfer A, Lu S, Bilello JP, Desrosiers RC, Edwards R, Raab-Traub N and Cullen BR: Epstein-Barr virus microRNAs are evolutionarily conserved and differentially expressed. PLoS Pathog *2*: e23, 2006.
6 Grundhoff A, Sullivan CS and Ganem D: A combined computational and microarray-based approach identifies novel microRNAs encoded by human gamma-herpesviruses. RNA *12*: 733-750, 2006.
7 Chen SJ, Chen GH, Chen YH, Liu CY, Chang KP, Chang YS and Chen HC: Characterization of Epstein-Barr virus miRNAome in nasopharyngeal carcinoma by deep sequencing. PloS one *5*: e12745, 2010.
8 Huang DP, Ho JH, Poon YF, Chew EC, Saw D, Lui M, Li CL, Mak LS, Lai SH and Lau WH: Establishment of a cell line (NPC/HK1) from a differentiated squamous carcinoma of the nasopharynx. Int J Cancer *26*: 127-132, 1980.
9 Glaser R, Zhang HY, Yao KT, Zhu HC, Wang FX, Li GY, Wen DS and Li YP: Two epithelial tumor cell lines (HNE-1 and HONE-1) latently infected with Epstein-Barr virus that were derived from nasopharyngeal carcinomas. Proc Natl Acad Sci USA *86*: 9524-9528, 1989.
10 Zhang Y, Gao HY, Feng HX, Deng L, Huang MY, Hu B, Cheng G, Wu QL, Cui NJ and Shao JY: Quantitative analysis of Epstein-Barr virus DNA in plasma and peripheral blood cells in patients with nasopharyngeal carcinoma. Zhonghua Yi Xue Za Zhi *84*: 982-986, 2004.
11 Yuan H, Yang BB and Xu ZF: The clinical value of quantitative analysis of plasma Epstein-Barr virus DNA in patients with nasopharyngeal carcinoma. Zhonghua Er Bi Yan Hou Ke Za Zhi *39*: 162-165, 2004.
12 Shotelersuk K, Khorprasert C, Sakdikul S, Pornthanakasem W, Voravud N and Mutirangura A: Epstein-Barr virus DNA in serum/plasma as a tumor marker for nasopharyngeal cancer. Clin Cancer Res *6*: 1046-1051, 2000.
13 Li B, Chen Z, Liu L, Huang Z, Huang Z and Xie S: Differences in sensitivity to HMME-mediated photodynamic therapy between EBV$^+$ C666-1 and EBV$^-$ CNE2 cells. Photodiagnosis Photodyn Ther *7*: 204-209, 2010.

Received April 22, 2012
Revised June 27, 2012
Accepted June 29, 2012